J Electroceram (2007) 18:339–346
DOI 10.1007/s10832-007-9171-x

Property-processing relationship in lead-free (K, Na, Li) NbO_3-solid solution system

Nader Marandian Hagh · B. Jadidian · A. Safari

Received: 12 October 2006 / Accepted: 9 May 2007 / Published online: 14 June 2007

Abstract There has been a significant driving force to eliminate the utilization, recycling, and disposal of ferroelectric ceramics with high content of toxic element (Pb). Recently, the ternary system of KNN-LT-LS has proven to be an outstanding lead-free piezoceramic with properties almost comparable to their lead-based counterpart, PZT. This study reports the effect of various processing conditions on the electromechanical properties of $(K_{0.44}Na_{0.52}Li_{0.04})(Nb_{0.84}Ta_{0.10}Sb_{0.06})O_3$ system. This includes powder processing, humidity, and exposure to oxygen rich environment during sintering. The Perovskite and Mixed-Oxide methods are used to prepare the stoichiometric powders. It will be shown that both processing methods are notably sensitive to the moisture of as received raw materials and the humidity of environment. Optimum results are obtained when the raw materials undergo a pre-heat treatment followed by formulating the desired composition in an inert atmosphere. The highest electromechanical properties are achieved when the ceramics are completely exposed to oxygen with a high flow rate. Sintered at 1150 °C for 1 h with an oxygen flow rate of 180 cm^3/min, the KNN-LT-LS ceramics prepared by Perovskite and Mixed-Oxide routes have $d_{33}\geq 300$ pC/N, $\varepsilon_{33}^T = 1865$, tan δ=0.02, k_{33}=0.65.

N. Marandian Hagh (✉) · A. Safari
Materials Science and Engineering Department,
Rutgers University, Piscataway, NJ 08854, USA
e-mail: nmhagh@rci.rutgers.edu

A. Safari
e-mail: safari@rci.rutgers.edu

B. Jadidian
J&W Medical LLC, 56 Partrick Rd.,
Westport, CT 06880, USA
e-mail: b.jadidian@jwmed.com

Keywords Lead-free piezoelectrics · Sodium potassium niobate · Processing-property relationship in ferroelectrics

1 Introduction

Lead-based piezoelectric materials such as lead zirconate titanate (PZT) are the most widely used piezoelectrics due to their superior piezoelectric performances [1, 2]. However its high content of toxic element (Pb>60 wt%) has triggered some concerns in Europe and Japan mainly due to the utilization, recycling, and disposal of lead-based ferroelectrics. Elimination of such issues has become a driving force for developing lead-free ferroelectric ceramics with properties almost comparable to their lead-based counterparts. Another motivation is to utilize such non-toxic ferroelectrics as transducers embedded in human body for therapeutic and monitoring applications.

Recently, potassium sodium niobate (KNN) ceramic has become attractive as a lead-free candidate due to a relatively high Curie temperature of ~420°C . However, KNN exhibits low piezoelectric properties (d_{33} of 80 pC/N and k_p of 36%) owing to the difficulty in being produced densely by conventional sintering process [3, 4]. This problem has been almost resolved by adding various additives either in the form of elements or compounds to KNN system [5–10]. Incorporation of $LiTaO_3$ into the Perovskite structure of $K_{0.5}Na_{0.5}NbO_3$ (KNN) has improved sinterability and consequently the piezoelectric properties [10]. Highest piezoelectric properties in (1-x) $K_{0.5}Na_{0.5}NbO_3$–x $LiTaO_3$ system has been achieved at the MPB region where x=5–6 mol%. Saito et al., has reported that introducing the $LiSbO_3$ (LS) along with $LiTaO_3$ (LT) to the KNN system is favorable due to the higher electronegativities of this B-site dopant [11]. Higher electronegativities of Ta^{5+} and Sb^{5+}

over the Nb^{5+} make the formed bonds more covalent than ionic. Hence the resultant Sp^3 hybridization of covalency over the ionic bond leads to further improvement in piezoelectric properties of KNN-LT-LS [11, 12]. Despite of higher electromechanical properties, the KNN-LT-LS system still requires to be carefully prepared. One of the main preparation issues arises from the formation of non-stoichiometric potassium niobate (KN) phases with hygroscopic nature [1]. This hygroscopic nature results in instability of the KN and hence KNN-LT-LS system. Besides the humidity issue, there is also a need for reliable processing route with high degree of reproducibility.

In this study, $(K_{0.44}Na_{0.52}Li_{0.04})(Nb_{0.84}Ta_{0.10}Sb_{0.06})O_3$ was prepared via two processing routes that we called the "Perovskite" and the "Mixed-Oxide" routes. In both we examined the effect of processing parameters on the electromechanical and dielectric properties of KNN-LT-LS to obtain an optimum processing condition. The parameters include humidity and sintering conditions. The former includes the effect of heat treatment of as received raw materials and mixing them either in laboratory environment or inside a glove box with argon gas flowing in it. The latter consists of the effect of oxygen flow rate and enclosure of the samples during sintering step.

2 Experimental procedures

2.1 Powder synthesis

The KNN-LT-LS powders were synthesized using two processing techniques, namely "Perovskite" and "Mixed-Oxide" routes. In the Perovskite route, first the binary compositions of sodium niobate ($NaNbO_3$; NN), potassium niobate ($KNbO_3$; KN), potassium tantalate ($KTaO_3$; KT), sodium antimonate ($NaSbO_3$; NS) and lithium antimonate ($LiSbO_3$; LS) were synthesized and then mixed together in order to form the final composition of $(K_{0.44}Na_{0.52}Li_{0.04})(Nb_{0.84}Ta_{0.10}Sb_{0.06})O_3$. Each binary Perovskite precursor was made by wet ball milling of appropriate molar ratio of K_2CO_3 (Alfa Aesar, 99.99% min.), Na_2CO_3 (Alfa Aesar, 99.95% min.), Nb_2O_5 (H.C. Starck, 99.9%), Li_2CO_3 (Alfa Aesar, 99.99% min.), Ta_2O_5 (Alfa Aesar, 99.99% min.) and Sb_2O_5 (Alfa Aesar, 99.99% min.) for 12 h in dry Acetone. The prepared binary powders were dried separately over night at 110°C in an oven and calcined at 800°C for 5 h. To determine the phase type of each binary Perovskite system, qualitative X-ray phase analysis was carried out using Philips D500 with Cu K_a radiation and a step-scan of 0.03 degrees per step in 2θ with 1 s dwell time. Then appropriate molar ratio of calcined NN, KN, KT, LS, and NS powders were mixed, ball milled in dry Acetone for 24 h, and dried over night at 110°C in an oven.

In the Mixed-Oxide method, the final composition was directly synthesized from the mixture of carbonate (Li_2CO_3, Na_2CO_3, and K_2CO_3) and oxide (Nb_2O_5, Ta_2O_5, Sb_2O_5) raw materials which were used in the form of as-received and heat treated (24 h at 220°C). The conditions of dry (Ar atmosphere) and humid (relative humidity of lab) atmospheres were employed in order to study the effect of relative humidity. Both synthesized powders were uniaxially pressed at 250 MPa pressure to form pellets with 12 mm diameter and 1.5 mm thickness. In the sintering step, ceramics were fired at 1150°C—1 h in covered (only with Pt foil) and uncovered conditions (direct exposure to sintering atmosphere) under the oxygen atmosphere. In order to study the effect of oxygen flow rate, prepared pellets were sintered under various oxygen flow rates of 80, 90, 100, 130, 180, 280, 360 cm^3/min.

The detailed specifications of each step (A to E) are as follows:

A: As received raw materials were processed in laboratory atmosphere (outside of glove box). Ceramic pellets were sintered in oxygen flow rate of 80 cm^3/min while their top and bottom surfaces were only covered with Pt foils.

B: As received raw materials were heat treated at 220°C for 24 h and powder precursors and pellets were prepared as described in procedure A.

C: As received raw materials were heat treated at 220°C for 24 h followed by preparing powder precursors in inert atmosphere (glove box). Pellets were sintered as described in step A.

D: Powder preparation was similar to the step C but top and bottom surfaces of pellets were in direct exposure to oxygen flow of 80 cm^3/min.

E: Powder processing is similar to step C, but pellets were sintered at higher oxygen flow rate (360 cm^3/min).

The microstructures of the sintered samples were studied by field emission scanning electron microscopy (FESEM) LEO (ZEISS) 982. Thermal etching of polished samples was performed at 1100°C for 30 min. Grain size measurements were carried out using the mean intercept length method from at least ten different areas of sample. The top and bottom surfaces of samples were lapped down to obtain 0.5 mm thick pellets. Then their either surface was coated with Au using a gold sputtering technique. The samples were poled at 30 kV/cm electric field for 15 min in a silicon oil bath at 100°C.

The relative permittivity ($\varepsilon_{33}^{T}/\varepsilon_0$) and dielectric loss were measured at room temperature and 1 kHz using an HP 4194A impedance/gain-phase analyzer (HP, Palo Alto, CA). Relative permittivity-temperature behavior of the samples were also measured during cooling ramp and data points were recorded every two degrees within the

temperature range of 30–380°C at 1 kHz. The room temperature polarization-field (*P–E*) hysteresis loops were measured with a Sawyer-Tower circuit that was operated at 50 Hz (Radiant Technologies Inc.).

Piezoelectric charge coefficient, d_{33}, was measured directly from a Berlincourt piezometer (Channel Products, Inc.) and also through the resonance and anti-resonance measurements. In the former method, at least ten readings from different locations of both top and bottom surfaces was made and averaged. Poisson's ratio was measured from the ratio of first overtone to fundamental resonance frequency ($f_s^{(2)}/f_s$) of the planar mode in accordance to the *IEEE* standards [13]. Piezoelectric planar, thickness, and the 31 mode coupling coefficients, (k_p, k_t, and k_{31}) were calculated from the resonance and anti-resonance frequencies of the impedance traces, based on the following relations and *IEEE* standards:

$$\frac{k_p^2}{1-k_p^2} = \frac{\Delta f\left[(\sigma^p)^2+\eta^2-1\right]}{f_s(1+\sigma^p)} \tag{1}$$

$$k_t^2 = \frac{\pi}{2}\frac{f_s}{f_p}\tan\frac{\pi}{2}\frac{\Delta f}{f_p} \tag{2}$$

$$\left(k_{31}^l\right)^2 = \frac{k_p^2(1-\sigma^p)}{2} \tag{3}$$

Where the f_s and f_p are the measured fundamental resonance and anti-resonances, σ^p is the Poisson's ratio and η is the frequency constant of a disk resonator. Longitudinal coupling coefficient, k_{33}, was estimated from the thickness and planar coupling coefficients [1]:

$$k_{33}^2 = k_p^2 + k_t^2 - k_p^2 k_t^2 \tag{4}$$

Using an HP 4194A impedance/gain-phase analyzer (HP, Palo Alto, CA), the planar mechanical quality factor was calculated using [13]:

$$Q_m = \frac{1}{R}\sqrt{\frac{L}{C_a}} \tag{5}$$

where the R, L, and C_a are the resistance, inductance and capacitance in the equivalent electrical circuit of the piezoelectric resonator.

3 Results and discussion

3.1 Microstructure and phase analysis

Microstructure analysis of bulk ceramics prepared from steps "E" of the Mixed-Oxide and Perovskite routes were carried out by scanning electron microscope (Fig. 1). As seen, the sharp-cornered cubic grains were observed on the top surfaces of as-sintered bodies. Similar grain morphology in potassium sodium niobate ($K_{0.5}Na_{0.5}NbO_3$) ceramics was also observed by Priya et al. [14]. The average relative density of the ceramics was ~97% with grain size of ~2.5 μm and 3 μm for Perovskite and Mixed-Oxide routes, respectively. The sintered samples of Perovskite route showed a uniform grain size distribution on their surfaces. However in the mixed oxide route, larger grains were distributed among smaller grains. The grain size range for both Perovskite and Mixed-Oxide were 2–10 μm.

Figure 1 also shows the fracture surface of the Perovskite and Mixed-Oxide route ceramics. In general, fracture in ceramics is initiated through the weak bonding. Once a crack nucleated, it grows along the path of weak bonding and eventually separates the solid into two pieces. In polycrystalline ceramics, the grain boundaries are the most possible path of weak connection where the second glassy phase and/or dislocations exist. The fracture in both processing routes occurred within the grains. The observed intra-granular fracture indicated that the bonds between two grains at grain boundaries were stronger than those within the grains. This also implies that the possibility of existing the glassy phase in grain boundaries is very low.

Phase analysis of ceramics prepared from step "E" of Perovskite and Mixed-Oxide routes were carried out by X-ray diffraction technique at room temperature (Fig. 2). Potassium niobate PDF # 77-1098 is used for X-Ray diffraction pattern fitting of these ceramics due to the unavailability of PDF pattern of KNN-LT-LS ternary system. Effect of polishing on the X-ray phase analysis of the ceramics was shown in Fig. 2(a). As-sintered sample showed the inversion in the intensity of the (011)–(100) and (022)–(200) planes, in regards to polished sample. This inversion in peak intensity could be due to the stress-induced domain switching during the polishing, similar to what has been reported in PZT ceramics [15]. According to X-Ray diffraction patterns in both processing techniques no second phase was detected. X-ray graphs of both techniques showed similar patterns which matched with orthorhombic structure [Fig. 2(b)]. However, Saito et al., has indicated that the room temperature phase was tetragonal [11, 12].

3.2 Perovskite route

In general, processing and preparation conditions determine the final properties of ceramics. Table 1 summarizes the properties of bulk ceramics made through the Perovskite route under the processing conditions of A to E. The samples prepared via procedure "A" showed a high dielectric loss (3.5%) and yielded poor electromechanical properties. By pre-heating of the as received raw materials at

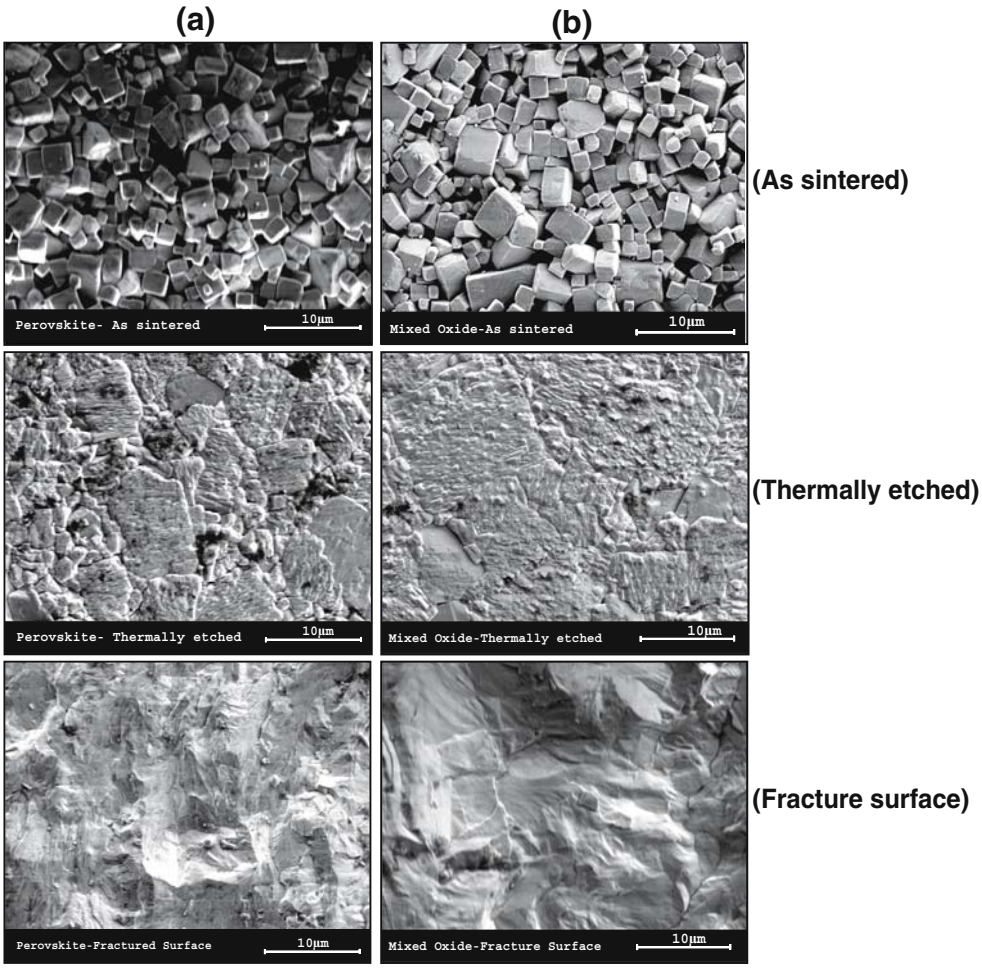

Fig. 1 Scanning electron microscopy (SEM) of as-sintered, thermally etched and fracture surface of (**a**) Perovskite and (**b**) Mixed-Oxide routes prepared from KNN-LT-LS ceramic sintered at 1150°C—1 h

220 °C (procedure "B") for 24 h, substantial changes in the properties were observed. Piezoelectric charge coefficient (d_{33}) and planar coupling coefficients (k_p) were improved by about 28% and 39%, respectively. Thickness mode of coupling coefficient (k_t) slightly increased and the longitudinal coupling coefficient (k_{33}) showed an improvement. In addition, room temperature permittivity increased while dielectric loss decreased. The importance of preheating of as received raw materials is mainly in acquiring the right stoichiometry by removing the excess adsorbed moisture. Among the used carbonate and oxide precursors, sodium carbonate (Na_2CO_3), lithium carbonates (Li_2CO_3), and antimony pent-oxide (Sb_2O_5) showed the highest sensitivity to the humidity. The measured weight losses after heat treatment at 220 °C for antimony pent-oxide, sodium carbonate, and lithium carbonate were about 4.5, 1.4, and 0.3%, respectively.

To prevent further exposure of raw materials to the humidity of laboratory environment, powder preparation was carried out in a glove box (step "C"). In comparison with the results obtained from procedure B, further improvement in piezoelectric charge and coupling coefficients were observed. Though the mechanical quality factor (Q_m) slightly declined.

Due to high vapor pressure of volatile oxides (such as Na_2O and K_2O), sintering of KNN-based ceramics are usually covered during sintering process [16]. This step is seemingly necessary to suppress evaporation of volatile species and formation of non-stoichiometry compounds within the ceramic. The covered (with Pt Foil) and uncovered (direct exposure to sintering atmosphere) samples had an insignificant difference in average weight loss after sintering. These were ~1.3 and 1.6%, respectively for covered and uncovered pellets. However, the results of step "D" and "E" showed that covering the KNN-LT-LS ceramics could be detrimental for the electromechanical properties of KNN-LT-LS ceramics. It was anticipated that the poor electromechanical properties in step "D" vs. "E" could be due to the oxygen deficiency in covered samples (Table 1). Oxygen vacancies as point defects could reduce the domain wall motion and act as pinning points [17]. This was accompanied by sharp decrease in coercive field (10.6 vs. 8.4 kV/cm) and increase in remnant polarization (14.3 vs. 18 μC/cm^2). The overall piezoelectric performance of the ceramics at high flow

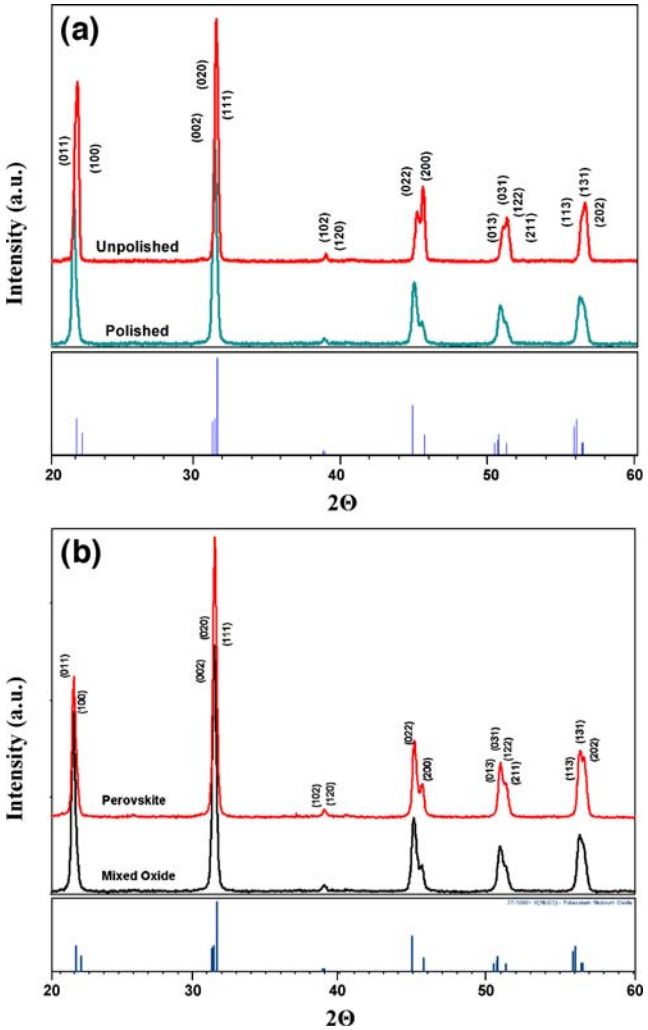

Fig. 2 X-Ray diffraction patterns of sintered ceramics prepared through the processing step of "E" based on Perovskite and mixed oxide routes. (**a**) Perovskite route polished and unpolished, (**b**) comparison between Perovskite and Mixed-Oxide routes after polishing

of oxygen were improved and average piezoelectric charge (d_{33}) and longitudinal coupling coefficients (k_{33}) were reached to ~300 pC/N and 61%, respectively (Step "E").

3.3 Mixed-Oxide route

In the Mixed-Oxide route, a similar trend in improvement of piezoelectric properties was observed (Table 2). Sensitivity of initial powder precursors to the humidity requires the careful preparation in controlled atmosphere otherwise it leads to poor electromechanical properties (step "A"). Careful preparation procedure including the preheating process along with preparation in a glove box (step "C") improved the room temperature permittivity while slightly changed the dielectric loss. The effect of higher oxygen flow on the properties of Mixed-Oxide prepared ceramics can be seen from the comparisons of steps D and E. Higher flow rates of oxygen led to higher coupling and piezoelectric coefficients in step E. Piezoelectric charge coefficient has a direct relationship with relative permittivity and remnant polarization based on [18, 19]:

$$d_{ij} \sim 2Q_{ij} \times K \times \varepsilon_o \times P_i \tag{6}$$

where d_{ij}, Q_{ij}, K, ε_o, and P_i are the piezoelectric charge coefficient, electrostriction coefficient, relative permittivity, the permittivity of free space, and the remnant polarization on poling, respectively. Assuming a negligible change in the electrostriction coefficient at temperatures below T_c (Curie point), the piezoelectric charge coefficient only depends upon the relative permittivity and remnant polarization. The higher remnant polarization and relative permittivity the higher piezoelectric charge coefficient. Improvement in remnant polarization (from A to E) accompanied the reduction of coercive field in both processing routes (Tables 1 and 2). Although the piezoelectric properties obtained were similar, the dielectric and polarization behaviors from steps "E" in both processing routes (Mixed-Oxide and Perovskite) differed. Higher relative permittivity and dielectric loss along with lower remnant polarization were observed in Perovskite route. It can be concluded that the Mixed-Oxide route is a suitable preparation technique since it eliminates the extra processing steps taken in Perovskite technique presented by Saito et al., [11, 12].

3.4 Effect of oxygen flow rate

As discussed above, the oxygen flow rate had a significant effect on the electromechanical properties of KNN-LT-LS samples. To obtain optimum oxygen flow rate, samples prepared via the step "E" of Perovskite route, were sintered in different oxygen flow rates of 80, 90, 100, 130, 180, 360, and >360 cm^3/min. Table 3 represents the properties of bulk ceramics after sintering at 1150°C—1 h. Due to the insufficient amount of the oxygen at flow rates <100 cm^3/min, the samples had lowest electromechanical properties. A notable improvement in piezoelectric properties was observed at the flow rate of 130–180 cm^3/min. However at flow rates of 360 cm^3/min and above, the properties were slightly declined.

Intrinsic and extrinsic effects in piezoelectrics influence the dielectric and piezoelectric behaviors of a piezoceramic. The intrinsic piezoelectric effect originates from the lattice deformation under the electric field while the extrinsic effect is an elastic deformation caused by domain walls and interfaces [20]. Effect of oxygen could be explained by extrinsic effect in piezoelectrics. Dielectric and piezoelectric properties of a ferroelectric are affected by domain wall motion. The former property is influenced by both 180° and non-180° domain wall motions and the latter property is only influenced by non-180° domain wall switching. In addition, the defined extrinsic response is related to the type and concentration of defects. As explained earlier in Perovskite

Table 1 Electromechanical properties of KNN-LT-LS ceramics obtained from *Perovskite* route under the different preparation conditions.

Property/processing step	A	B	C	D	E
ε_{33}^{T}(1 kHz at RT)	745	890	1360	1540	1740
tan δ (1 kHz at RT), %	3.5	2.8	3.3	2.5	2.1
d_{33} (pC/N)	145	185	210	220	300
k_p	0.280	0.390	0.392	0.374	0.468
k_t	0.270	0.281	0.372	0.404	0.438
k_{33}	0.410	0.489	0.52	0.533	0.609
k_{31}	0.140	0.220	0.224	0.204	0.253
Q_m	85	82	75	62	53
P_r ($\mu C/cm^2$)	13.8	13.1	14.1	14.3	18.0
E_c (kV/cm)	13.3	12.1	11.0	10.6	8.4

A: As received raw materials were prepared in laboratory atmosphere without heat treating the powder precursors. Ceramic pellets were covered with Pt foils and sintered in oxygen flow rate of 80 cm^3/min. *B:* As received raw materials were heat treated at 220 °C for 24 h and powder precursors and pellets were prepared as described in procedure A. *C:* As received raw materials were heat treated at 220°C for 24 h followed by preparing powder precursors in inert atmosphere (glove box). Pellets were sintered as described in step A. *D:* Powder preparation was similar to the step C but top and bottom surfaces of pellets were in direct exposure to oxygen flow of 80 cm^3/min. *E:* Powder processing is similar to step C, but pellets were sintered at higher oxygen flow rate (360 cm^3/min).

section, common point defects namely oxygen vacancies could form during sintering, act as pinning points, and reduce the domain wall motions. The resistance in domain wall motion led to higher coercive fields (Tables 1 and 2). This in turn resulted in poor piezoelectric and dielectric properties. On the other hand, high oxygen flow rates (130–180 cm^3/min) facilitated domain wall switching and gave rise to higher polarizability level with lower coercive field. However, at very high oxygen flow rates (≥360 cm^3/min), the cause for slight decrease in piezoelectric and dielectric properties is not quite clear and requires more study.

3.5 Dielectric behavior of KNN-LT-LS ceramics

Temperature dependency of relative permittivity and dielectric loss was carried out for KNN-LT-LS samples prepared by processing steps "E" of Perovskite and Mixed-Oxide routes. Shown in Fig. 3 are data points collected during cooling in the temperature range of 30–380°C. The Curie point (T_c) (cubic-tetragonal phase transition) for Perovskite and Mixed-Oxide routes were 266 and 264°C, respectively.

Maximum relative permittivity for Mixed-Oxide samples was higher than that of Perovskite ones (8940 vs. 8540). Although, the dielectric losses in both routes were minimum at their Curie points, however their values rapidly increased at $T>T_c$ which representing the conductive nature of these ceramics. The second phase transition, the orthorhombic to tetragonal, occurred at slightly above room temperatures, 44°C for Perovskite and 34°C for Mixed-Oxide routes. This indicated that the orthorhombic phase existed at room temperature for both preparation techniques. However Saito et al. [11] reported the existence of tetragonal phase at room temperature and T_c=254°C. These dissimilarities are attrib-

Table 2 Electromechanical properties of KNN-LT-LS ceramics obtained from *Mixed-Oxide* route under the different preparation conditions.

Property/processing step	A	C	D	E
ε_{33}^{T}(1 kHz at RT)	665	1350	1570	1590
tan δ (1 kHz at RT), %	2.9	3.0	1.6	1.7
d_{33} (pC/N)	155	175	225	297
k_p	0.220	0.223	0.419	0.442
k_t	0.284	0.290	0.345	0.446
k_{33}	0.350	0.360	0.523	0.596
k_{31}	0.120	0.130	0.229	0.243
Q_m	85	85	74	73
P_r ($\mu C/cm^2$)	13.2	18.5	19.3	21.9
E_c (kV/cm)	12.1	11.73	10.2	8.2

A: As received raw materials powder precursors were prepared out side of glove box without heat treating. Ceramic pellets were covered with Pt foils and sintered in oxygen flow rate of 80 cm^3/min. *C:* As received raw materials were heat treated at 220°C for 24 h followed by preparing powder precursors in inert atmosphere (glove box). Pellets were sintered as described in step A. *D:* Powder preparation was similar to the step C but top and bottom surfaces of pellets were in direct exposure to oxygen flow of 80 cm^3/min. *E:* Powder processing is similar to step C, but pellets were sintered at higher oxygen flow rate (360 cm^3/min).

Table 3 Effect of oxygen flow rate on the electromechanical properties of KNN-LT-LS ceramics prepared by *Perovskite* route.

Property	O_2 Flow Rate (cm^3/min)						
	80	90	100	130	180	360	>360
d_{33} (pC/N)*	210	220	190	300	315	300	285
d_{33} (pC/N)**	205	210	190	293	299	272	268
ε_{33}^{T} (1 kHz at RT)	1640	1685	1480	1865	1865	1710	1710
tan δ (1 kHz at RT), %	2.6	3.0	3.0	2.2	2.1	2.0	2.3
k_p	0.361	0.358	0.313	0.487	0.484	0.480	0.458
k_t	0.398	0.313	0.256	0.461	0.497	0.394	0.421
k_{33}	0.517	0.462	0.396	0.632	0.650	0.592	0.594
k_{31}	0.198	0.195	0.170	0.265	0.263	0.263	0.247
Q_m	64	59	61	52	50	51	54

*Measured by Berlincourt piezometer
**Calculated via resonance/anti-resonance technique using IEEE standard

uted to the possibility of a slight compositional difference between this study and Saito's work.

3.6 Polarization-field behavior

Polarization-filed (P–E hysteresis loop) behavior of the ceramics prepared through the processing steps "E" of both Perovskite and Mixed-Oxide routes are depicted in Fig. 4. The mixed oxide route samples had higher remnant polarization than the Perovskite samples. At 30 kV/cm electric field, the remnant polarization (P_r) and coercive field (E_c) of the Mixed-Oxide were ~22 μC/cm^2 and ~8.2 kV/cm, respectively. Since the Perovskite route showed slightly higher piezoelectric charge and coupling coefficients than mixed oxide route, it was expected that their remnant polarization to be higher. However one should consider the relative permittivity effect on polarization besides the piezoelectric coefficient. Based on the Eq. 6 the polarization could be written as:

$$P_i \sim \frac{d_{ij}}{K \times \varepsilon_0 \times 2Q_{ij}} \tag{7}$$

Considering negligible changes in electrostriction coefficient (Q_{ij}) of Perovskite and Mixed-Oxide ceramics, the remnant polarization mainly would depend on relative permittivity and piezoelectric coefficient. Since the d_{33} of

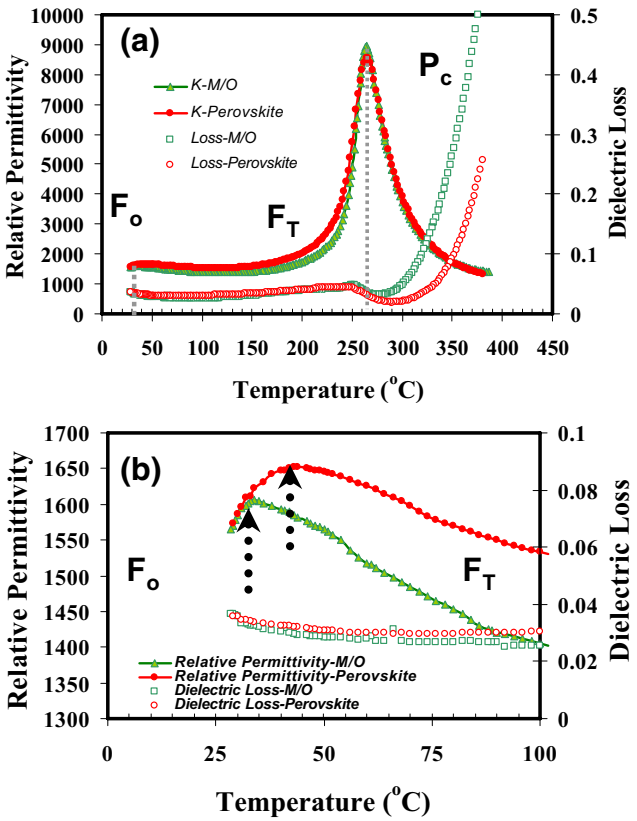

Fig. 3 (**a**) Relative permittivity and dielectric loss behavior of KNN-LT-LS ceramics prepared from two different processing techniques (Perovskite and M/O: Mixed oxide route). (**b**) Relative permittivity and dielectric loss behavior of KNN-LT-LS ceramics prepared from two different processing routes near orthorhombic-tetragonal phase transition

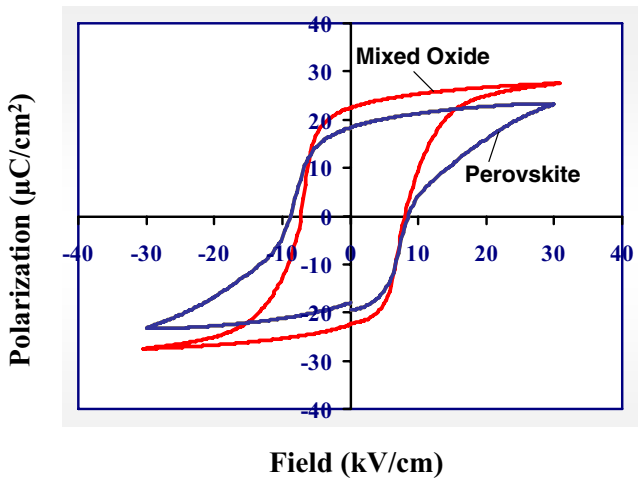

Fig. 4 Polarization-field hysteresis loop of Perovskite and Mixed-Oxide route ceramics prepared through the processing step "E"

both systems were almost similar, therefore higher remnant polarization observed in Mixed-Oxide ceramics could justify their lower relative permittivity (compare Tables 1 and 2). In the mean time, we also need to consider the slight shifting of the transition temperature (orthorhombic–tetragonal) in Mixed-Oxide route toward room temperature, which this could affect the remnant polarization in Mixed-Oxide system.

4 Conclusion and summary

To find the optimum processing conditions, the effect of different oxygen flow rate and humidity were investigated in KNN-LT-LS ceramics prepared by Perovskite and Mixed-Oxide routes. In Perovskite route, the samples were prepared based on pre-calcination of binary components while Mixed-Oxide route was a direct synthesis of final composition through oxide/carbonate raw materials. Samples made in the laboratory environment yielded different electromechanical properties than those prepared in an inert atmosphere (Ar). In fact, the sensitivity of both preparation techniques to the humidity of environment implied that a controlled atmosphere during the powder processing step was necessary. In both preparation techniques, the inert atmosphere improved piezoelectric properties. It was found that the presence of high oxygen flow rate along with direct exposure were crucial to obtain higher piezoelectric properties. The optimum properties were obtained in the oxygen flow rate of 130–180 cm^3/min. It is anticipated that reduction in oxygen vacancies by providing higher oxygen flow rates facilitated domain wall switching and led to higher remnant polarization with lower coercive field.

The average value for piezoelectric charge and longitudinal coupling coefficients for Perovskite route at the flow rate of 180 cm^3/min was 315 pC/N and 65%, respectively. Both preparation techniques yielded similar electromechanical properties and Curie temperatures. While the second phase transition temperatures were found to be slightly different, Mixed-Oxide route samples had lower dielectric loss and relative permittivity at room temperature. It can be concluded that the Mixed-Oxide route is a suitable preparation technique since it eliminates the extra processing steps taken in Perovskite technique. High electromechanical properties such as $d_{33} \geq 300$ pC/N and k_{33} of 0.65 make the KNN-LT-LS composition as an excellent candidate for lead-free piezoelectric applications.

Acknowledgements The financial support of Glenn Howatt Foundation at the Electroceramic Laboratory of Rutgers University is acknowledged.

References

1. B. Jaffe, *Piezoelectric Ceramics* (Academic, New York, 1971), p. 214
2. J.F. Tressler, S. Alkoy, R.E. Newnham, J. Electroceram. **2**(4), 257 (1998)
3. L. Egerton, D.M. Dillon, J. Am. Ceram. Soc. **42**, 438 (1959)
4. R.E. Jaeger, L. Egerton, J. Am. Ceram. Soc. **45**, 209 (1962)
5. M. Kosec, D. Kolar, Mater. Res. Bull. **10**, 335 (1975)
6. S. Tashiro, H. Nagamatsu, K. Nagata, Jpn. J. Appl. Phys. **41**, 7113 (2002)
7. V. Bobnar, B. Malic, J. Holc, M. Kosec, J. Appl. Phys. **98**, 024113 (2005)
8. M. Matsubara, T. Yamaguchi, K. Kikuta, S. Hirano, Jpn. J. Appl. Phys. **43**, 7159 (2004)
9. M. Matsubara, T. Yamaguchi, K. Kikuta, S. Hirano, Jpn. J. Appl. Phys. **44**, 258 (2005)
10. Y. Guo, Ken-ichi Kakimoto, H. Ohasto, Matt. Lett. **59**, 241 (2005)
11. Y. Saito, H. Takao, T. Tani, T. Nanoyama, K. Takatori, T. Homma, T. Nagaya, M. Nakamura, Nature **123**, 84 (2004)
12. T. Nonoyama, T. Nagaya, Y. Saito, K. Takatori, T. Homma, H. Takao, US Patent #0178605A1, (2003)
13. The Institute of Electrical and Electronics Engineers (IEEE), Standards on Piezoelectricity, American National Standards Institute, ANSI/IEEE Std. 176, (1987)
14. S. Priya, A. Ando, K. Uchino, *Development in Dielectric Materials and Electronic Devices*, Ceramic Trans, ed. By K.M. Nair, R. Guo, A.S. Bhalla, S.I. Hirano,D. Suvorov (The American Ceramic Society, Indianapolis, 2005), p. 223
15. Y. Saito, Jpn. J. Appl. Phys. **36**, 5963–5996 (1997)
16. K. Kakimoto, I. Masuda, H. Ohsato, J. Euro. Ceram. Soc. **25**, 2719 (2005)
17. F. Xia, X. Yao, J. Mater. Res. 14, 1683 (1999)
18. S.E. Park, T. Shrout, IEEE Trans. Ultrason. Ferroelectr. Freq. Control **44**, (1997)
19. T.R. Shrout, R. Eitel, C. Randall, *Piezoelectric Materials in Devices*, ed. By N. Setter (EPFL Swiss Federal Institute of Technology, Lausanne, Switzerland, 2002), p. 413
20. F. Xia, X. Yao, J. Appl. Phys. **92**, 2709 (2002)